inorganics

MDPI

Review

Recent Progress of Carbon Dots in Fluorescence Sensing

Xiao-Tian Lou [1,2], Lei Zhan [3,*] and Bin-Bin Chen [2,*]

[1] Faculty of Science and Engineering, University of Nottingham Ningbo China, Ningbo 315100, China; shyxl8@nottingham.edu.cn
[2] School of Chemistry & Molecular Engineering, East China University of Science and Technology, Shanghai 200237, China
[3] Key Laboratory of Luminescence Analysis and Molecular Sensing, Ministry of Education, College of Pharmaceutical Science, Southwest University, Beibei, Chongqing 400715, China
* Correspondence: zhanlei6@swu.edu.cn (L.Z.); binbinchen@ecust.edu.cn (B.-B.C.)

Abstract

Carbon dots (CDs) have attracted much attention as new types of luminescent carbon nanomaterials in recent years because of their tunable fluorescence, good biocompatibility, high stability, and low cost. In this review, the classification of CDs is overviewed based on their differences in structure. Subsequently, the latest research progress of CDs in fluorescence sensing is systematically summarized and various sensing principles are elucidated in detail, including fluorescence resonance energy transfer, aggregation-induced emission, aggregation-caused quenching, electron transfer, and the inner filter effect. Finally, the challenges and future direction of CD fluorescent probes are discussed in detail. The purpose of this review is to stimulate the design of advanced CD fluorescent probes and achieve the accurate and reliable measurement of analytes in complex samples.

Keywords: carbon dots; structural classification; fluorescence sensing; detection mechanism; a review

check for updates

Academic Editor: Kazuyuki Takahashi

Received: 1 July 2025
Revised: 26 July 2025
Accepted: 29 July 2025
Published: 31 July 2025

Citation: Lou, X.-T.; Zhan, L.; Chen, B.-B. Recent Progress of Carbon Dots in Fluorescence Sensing. *Inorganics* **2025**, *13*, 256. https://doi.org/10.3390/inorganics13080256

Copyright: © 2025 by the authors. Licensee MDPI, Basel, Switzerland. This article is an open access article distributed under the terms and conditions of the Creative Commons Attribution (CC BY) license (https://creativecommons.org/licenses/by/4.0/).

1. Introduction

Carbon dots (CDs) have garnered widespread attention as a novel class of zero-dimensional carbon nanomaterials, owing to their tunable emission properties, superior chemical stability, excellent biocompatibility, and cost-effectiveness [1–5]. Owing to these distinctive advantages, CDs have been extensively applied in diverse fields including chemicals and biosensing, in vivo imaging, photothermal/photodynamic therapy, and photocatalysis. Currently, the formation of CDs can be achieved through the chemical or physical fragmentation of bulk carbon materials (termed "top-down" approaches) [6–8], as well as the thermal polymerization of organic molecular or biomass precursors (termed "bottom-up" strategies) [9–11]. However, the diversity of precursors and synthesis conditions, coupled with the ambiguous formation mechanisms, result in CDs with intricate structures that are challenging to characterize unambiguously. In current research, CDs are broadly classified into distinct categories based on structural disparities: fully disordered carbon nanoclusters (CNCs), highly carbonized carbon nanodots (CNDs), partially crystalline carbonized polymer dots (CPDs), highly crystalline carbon quantum dots (CQDs), and graphene quantum dots (GQDs) [12,13].

Fluorescence is a ubiquitous photoluminescence phenomenon. When fluorescent materials are irradiated by excitation light of specific wavelengths, they absorb incident photon energy, promoting electrons to an excited state. Subsequent radiative relaxation of

these excited electrons back to the ground state instantaneously generates emitted light with a longer wavelength than the incident light, a process defined as fluorescence [14]. Traditional fluorescent materials primarily include inorganic fluorescent materials (e.g., semiconductor quantum dots (QDs) and lanthanide compounds) and organic fluorescent materials (e.g., dye molecules and polymer dots). While inorganic QDs exhibit intrinsic toxicity due to the presence of heavy metal ions, organic dyes are often limited by poor aqueous solubility and high production costs. In contrast, CDs, as novel luminescent carbon-based nanoprobes, demonstrate distinct advantages in fluorescence sensing applications [15]: (i) Excellent aqueous solubility. CDs are enriched with hydrophilic functional groups (e.g., hydroxyl and carboxyl groups) on their surfaces, enabling their effective utilization in solution-phase sensing. (ii) High quantum yields (QYs). CDs exhibit QYs approaching 100%, satisfying the requirements of diverse fluorescence sensing systems. (iii) Superior biocompatibility. Owing to their metal-free composition, CDs demonstrate low cytotoxicity, making them ideal for cellular or in vivo imaging applications. (iv) Exceptional photostability. The fluorescence intensity of CDs remains stable under prolonged UV irradiation, facilitating long-term optical tracking. Consequently, compared to conventional semiconductor QDs and fluorescent dyes, CDs exhibit enhanced biocompatibility, lower production costs, superior aqueous solubility, and robust anti-photobleaching properties, which collectively drive their widespread exploration in fluorescence sensing technologies.

In this review, the fundamental properties of CDs including their composition, structural configurations, and classification are summarized. Subsequently, recent advancements in CDs-based fluorescence sensing are systematically reviewed, with further elaboration on their fluorescence sensing mechanisms including fluorescence resonance energy transfer (FRET), aggregation-induced emission (AIE), aggregation-caused quenching (ACQ), electron transfer (ET), and the inner filter effect (IFE). Finally, future research directions and critical challenges for CDs in fluorescence sensing are comprehensively discussed. The purpose of this review is not only to consolidate the latest progress in CDs-enabled fluorescence sensing but, more importantly, to inspire the rational design of advanced CDs-based fluorescent probes. Such innovations aim to achieve reliable and precise quantification of analytes in complex matrices, thereby bridging the gap between laboratory research and real-world applications.

2. Overview of CDs

2.1. Fundamental Composition

CDs, recognized as a novel class of luminescent carbon nanoparticles, are predominantly composed of carbon. Those consisting solely of carbon and oxygen are termed "bare" CDs, representing the simplest structural configuration. These "bare" CDs can be synthesized via the chemical oxidation of large-sized carbon materials, typically exhibiting surfaces functionalized exclusively with oxygen-containing groups such as hydroxyl, carbonyl, or carboxyl moieties. However, the carboxyl groups on the surface of "bare" CDs induce non-radiative recombination of electron–hole pairs [16], significantly diminishing their QYs and thereby severely limiting practical applicability. Moreover, the homogeneity of surface chemical groups restricts their functional versatility. Consequently, these early-developed "bare" CDs face substantial challenges in achieving widespread utilization.

Surface passivation strategies have proven effective in enhancing the luminescence efficiency of CDs by stabilizing emissions originating from surface energy traps [17]. Inspired by this approach, a series of functionalization strategies—including surface modification and heteroatom doping—have been developed to improve both the optoelectronic performance and structural integrity of CDs [18]. Heteroatom doping introduces non-metal (e.g., nitrogen, phosphorus, silicon) or metal (e.g., magnesium, copper, lanthanides) ele-

ments into the CDs' framework, altering their compositional profile, redistributing electron density, and tailoring optoelectronic properties. In addition, surface modification grafts functional groups or bioactive molecules onto CDs' surfaces, enriching their chemical reactivity and creating analyte-specific binding sites. Together, these strategies not only refine the structural and functional attributes of CDs but also endow them with unique photophysical features.

2.2. Structure and Classification

The structural complexity of CDs arises from the carbonization or polymerization of reaction precursors, forming core structures adorned with diverse surface chemical groups. Typically, the carbon core comprises sp^2/sp^3 hybridized carbon, while the surface is functionalized with chemical moieties or polymer chains, forming a carbon shell. Extensive studies reveal that the carbon core predominantly adopts either graphitic crystalline lattices or amorphous carbon configurations [19–21]. The core structure critically influences both the optical properties and photostability of CDs [22], with graphitic lattice-dominated CDs generally exhibiting superior resistance to photobleaching compared to their amorphous counterparts. However, surface chemical functionalization governs aqueous dispersibility and modulates the optical bandgap. Based on structural distinctions, CDs can be classified into five subtypes (Figure 1) [12]: (i) Highly disordered CNCs lacking defined carbon cores or crystallinity; (ii) CPDs featuring polymer/carbon hybrid architectures with carbon cores and extensive surface polymer chains/functional groups; (iii) highly carbonized CNDs possessing discernible carbon cores but lacking crystallinity, with limited surface functionalization; (iv) highly crystalline CQDs exhibiting well-defined lattice fringes and abundant surface functional groups; and (v) single- or few-layer GQDs characterized by graphene-like lattice structures with edge or interlayer defects incorporating chemical functionalities.

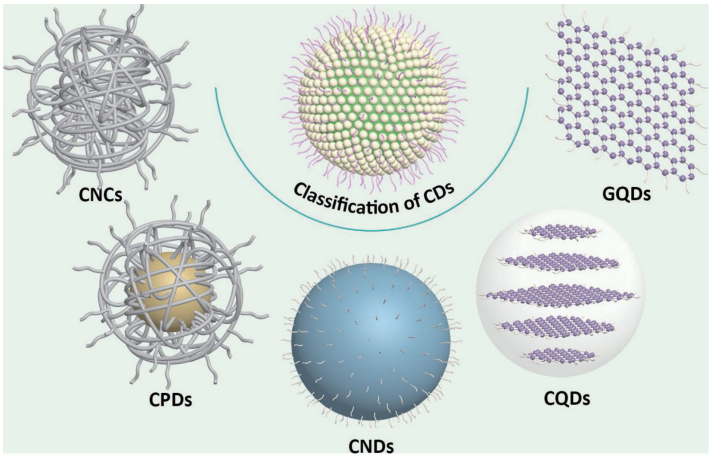


Figure 1. The classification of carbon dots (CDs). CNCs, carbon nanoclusters; CPDs, carbonized polymer dots; CNDs, carbon nanodots; CQDs, carbon quantum dots; GQDs, graphene quantum dots [12]. Reprinted with permission from Ref. [12]. Copyright 2023 Springer Nature.

CDs typically support multiple allowed electronic transitions [23], including $\sigma \rightarrow \sigma^*$, $\sigma \rightarrow \pi^*$, $n \rightarrow \sigma^*$, $\pi \rightarrow \pi^*$, and $n \rightarrow \pi^*$ transitions, which are intrinsically linked to their structural and optical characteristics. Aromatic sp^2 domains within the carbon core contribute to π states, while n states originate from surface functional groups containing lone electron pairs.Notably, electronic transitions from n states in sp^2-hybridized surface functionalities to π^* states in the aromatic carbon framework may occur. Consequently, electronic structure and associated transitions profoundly impact optical properties; however, the inherent complexity and variability in CDs composition and architecture pose significant challenges to the definitive elucidation of their electronic structures.

2.3. Optical Properties

2.3.1. Light Absorption Properties

CDs exhibit strong optical absorption spanning from the UV region into the visible and even near-infrared (NIR) spectral ranges. Figure 2 illustrates the correlation between electronic transitions and absorption spectra in CDs [24]. The carbon core represents the sp^2-conjugated domains within the CDs interior, while the carbon shell refers to the surface chemical groups. Generally, short-wavelength absorption below 300 nm (Figure 2, Band I) corresponds to $\pi \rightarrow \pi^*$ transitions (C=C bonds) in aromatic sp^2 carbon clusters, whereas absorption between 300 and 400 nm (Figure 2, Band II) is attributed to $n \rightarrow \pi^*$ transitions of C=O bonds in the carbon core [25–31]. Absorption bands above 400 nm (Figure 2, Bands III–V) arise from surface state transitions involving lone electron pairs [27–29]. Notably, an increased content of graphitic nitrogen or oxygen-containing functional groups induces a redshift in CQD absorption. It is noteworthy that the broad surface state absorption band and $n \rightarrow \pi^*$ transitions typically overlap rather than exist in isolation, minimizing interference with emission tunability and enabling smooth color gradients with varying excitation wavelengths [28]. Additionally, the low-energy absorption band near 300 nm originates from $n \rightarrow \pi^*$ and $\pi \rightarrow \pi^*$ charge transfer transitions or interlayer charge transfer processes with dominant $\pi \rightarrow \pi^*$ contributions [26].

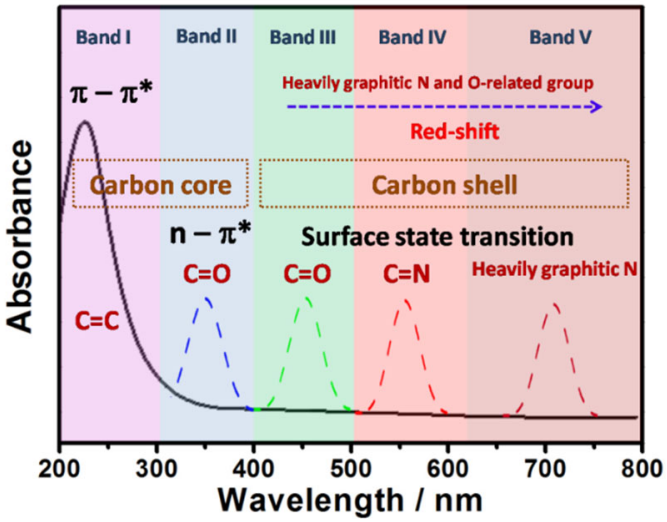


Figure 2. A schematic illustration of the relationship between the absorption spectrum and electron transition of CDs [24]. Reprinted from Ref. [24].

2.3.2. Fluorescence Origin

A thorough understanding of the fluorescence mechanisms in CDs is crucial for guiding their synthesis. Despite extensive research efforts, the luminescence origins of CDs remain poorly elucidated due to the complex compositions and structures of CDs derived from diverse precursors and synthetic methodologies. Reported optical mechanisms can be broadly categorized into two classes: core-related emissions and surface-related emissions [32–34]. Core-related emissions are further subdivided into quantum confinement effects, conjugated structures, and free zigzag sites, while surface-related emissions encompass crosslink-enhanced emission, surface/edge defects, and multiple emission centers. Generally, interpretations of CD fluorescence mechanisms must be tailored to their specific structural features, as the development of a universal conceptual framework to comprehensively explain CD luminescence remains highly challenging.

3. Fluorescence Sensing Applications

3.1. FRET

FRET occurs when the emission spectrum of an energy donor overlaps with the absorption spectrum of an energy acceptor, and the donor–acceptor distance is less than 10 nm [15]. Specifically, upon absorbing incident light energy, electrons in the donor are excited to a higher energy state. Before these excited electrons return to the ground state, their energy is transferred to the adjacent acceptor via dipole–dipole interactions (i.e., resonance energy transfer). This intermolecular electric dipole interaction enables non-radiative energy conversion, where the donor's fluorescence intensity decreases as energy is transferred to the acceptor. The efficiency of energy transfer is critically dependent on the spectral overlap between the donor's emission and acceptor's absorption, the relative orientation of donor–acceptor dipoles, and their distance.

In FRET-based sensing systems, electron-rich CDs often serve as energy donors [35–37]. For instance, Cyriac et al. report a CD-based FRET sensor for selective ammonia gas detection [38], wherein CDs act as the signal transducer and sodium lipoate as the recognition molecule. Ammonia exposure induced structural changes in sodium lipoate, activating FRET from CDs to sodium lipoate and enabling specific ammonia detection (Figure 3). The sensor exhibited a linear range of 0–200 ppm and a detection limit as low as 3 ppm. The authors further demonstrated selective ammonia vapor detection using cotton fibers coated with the sensor solution. Ratiometric fluorescent probes, which incorporate self-calibrating capabilities, effectively mitigate false signals or instability caused by environmental fluctuations, thereby enhancing detection reliability and sensitivity. Building on this principle, Pina-Luis et al. developed a CD-based FRET system for riboflavin detection [39], employing CDs as the energy donor and riboflavin as the acceptor. The fluorescence ratio signal shows a linear correlation with riboflavin concentrations (0–11 μM) and achieves a detection limit of 0.025 μM. This riboflavin assay offers advantages of rapidity, cost-effectiveness, high sensitivity, and selectivity, with potential applicability in biological and food samples. Table 1 summarizes representative CDs-based FRET sensing systems for detecting analytes such as metal ions, cysteine, and hyaluronic acid.

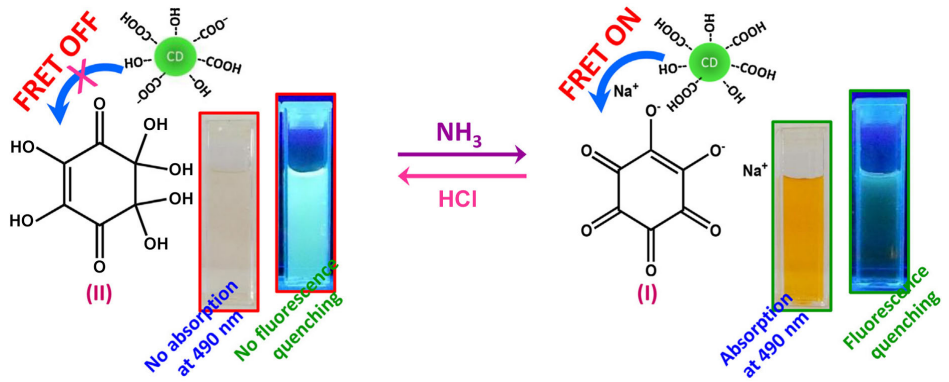


Figure 3. Schematic illustration of the detection of ammonia [38]. Reproduced from Ref. [38] with permission from Elsevier.

Table 1. Summary of CD detection based on FRET mechanism.

Analytes	Linearity Range	Limit of Detection	Reference
Ag^+	0–115.2 μM	250 nM	[40]
Cysteine	0–60 μM	100 nM	[41]
2, 6-Dipyridinic acid	0.1–750 nM	0.1 nM	[42]
Hyaluronidase	0.1–8 U/mL	0.05 U/mL	[43]
Dichlorvos	0.05–100 nM	0.019 nM	[44]

3.2. AIE

The concept of AIE is first proposed by Tang et al. in 2001 during investigations of the optical properties of 1-methyl-1,2,3,4,5-pentaphenylsilane [45]. AIE-active materials exhibit restricted intramolecular motion upon aggregation, leading to a transition from non-radiative to radiative decay pathways and thereby significantly enhancing optical emission intensity. Sensors based on AIE materials generate "turn-on" optical output signals, which minimize false-positive results and improve detection sensitivity.

In recent years, CDs with AIE properties have been developed, enabling the precise quantification of trace analytes. For example, Guo et al. designed a CDs@$[Ru(bpy)_3]^{2+}$ sensing platform for fluoride ion (F^-) detection [46]. Specifically, aluminum ion (Al^{3+}) triggered AIE-active CDs served as the responsive signal, while red-emitting $[Ru(bpy)_3]^{2+}$ complexes acted as the reference signal (Figure 4). As F^- concentration increased, the ratiometric probe exhibited a continuous fluorescence color transition from red to cyan. The sensor demonstrated a linear detection range of 0–450 μM for F^- ions, with a detection limit of 1.53 μM. The authors successfully applied this platform for rapid F^- quantification in water and toothpaste samples, achieving satisfactory reproducibility and relative standard deviations.

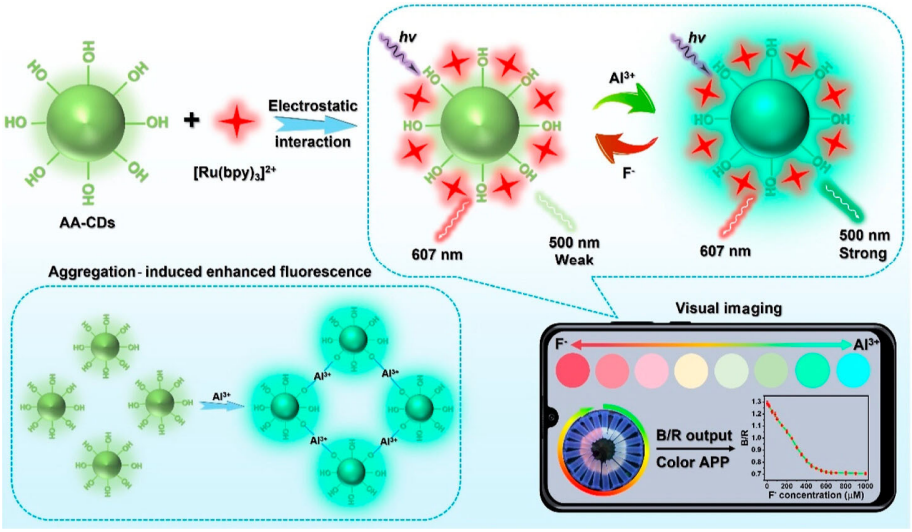


Figure 4. Portable smartphone platform based on AIE CDs for ratiometric visual sensing [46]. Reprinted with permission from Ref. [46]. Copyright 2023 American Chemical Society.

This platform offers advantages of low cost, robust stability, excellent selectivity, and reproducibility, serving as a powerful tool for smartphone-based microsensor platforms enabling visual quantitative detection. Concurrently, Wu et al. synthesized AIE-active CDs using tea saponin for human serum albumin (HSA) detection [47]. HSA introduction induces fluorescence enhancement in the CDs, exhibiting a linear regression across the 0–180 μM concentration range. Furthermore, the CDs demonstrate mitochondrial targeting capability in live cells for intracellular HSA detection, underscoring their potential in biosensing applications.

3.3. ACQ

ACQ is a prevalent phenomenon in fluorescent materials, wherein the energy of excited fluorophores is rapidly transferred to ground state counterparts without radiative decay, resulting in reduced or quenched fluorescence emission [48,49]. CDs, particularly GQDs, are highly susceptible to ACQ due to their atomically thin structures and significant spectral overlap between emission and absorption bands [50].

CD aggregation often induces fluorescence quenching, providing a foundation for designing fluorescent sensing systems. For instance, Jelinek et al. develop an ascorbic acid-based hydrogel sensor encapsulating fluorescent CDs for reactive oxygen species (ROS) detection [51]. The sensing mechanism relies on ROS-induced oxidation of ascorbate units within the hydrogel matrix, causing framework collapse, CD aggregation, and subsequent luminescence quenching (Figure 5). The CD/hydrogel platform demonstrates high sensitivity for chemically generated ROS detection in both solution and live cellular environments, with a linear range of 10–100 nM. Similarly, Wang et al. report a CD-based ACQ strategy for highly sensitive and selective cobalt ion (Co^{2+}) detection [52]. Co^{2+} binding to nitrogen donor atoms on CDs induces particle aggregation and fluorescence quenching. This sensor exhibits a linear response from 10 nM to 5 μM and a detection limit of 2 nM. Notably, the CDs display excellent biocompatibility and photostability, enabling specific Co^{2+} detection and real-time visualization of Co^{2+}-induced physiological changes in A549 cells.

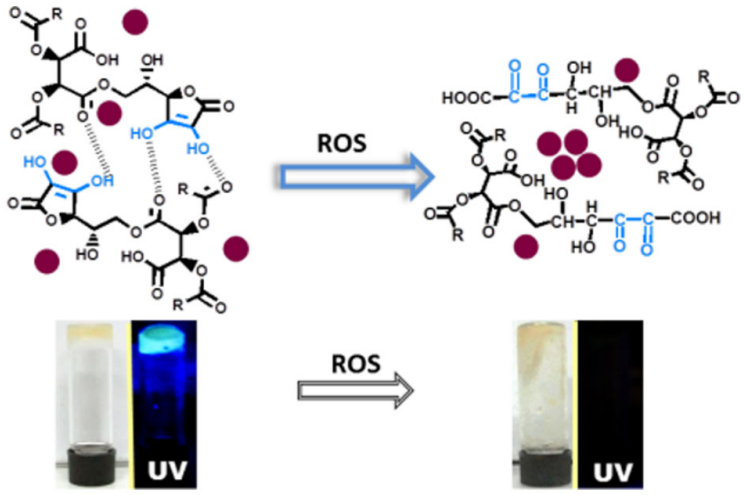


Figure 5. Illustration of the ROS detection [51]. Reprinted with permission from Ref. [51]. Copyright 2017 American Chemical Society.

3.4. ET

ET refers to the process wherein excited electrons from a donor are transferred to an acceptor under illumination. CDs, typically acting as electron donors, generate excited-state electrons upon light irradiation, which are subsequently transferred to acceptors, resulting in reduced or quenched CD fluorescence. Leveraging this principle, Wu et al. synthesize CDs with unique hydrophilic functional groups and graphitic nitrogen via polymerization and carbonization of a novel norfloxacin precursor bearing heterocyclic structures for radioactive uranyl (UO_2^{2+}) ion detection [53]. Strong coordination interactions between CDs and UO_2^{2+} ions enable effective fluorescence quenching (Figure 6). Detailed experiments confirm that the quenching mechanism arises from ET, with a linear range of 0–10 μM and a detection limit of 20.38 nM. The authors further develop a solid-phase sensing technology for rapid UO_2^{2+} detection in environmental samples.

Additionally, Li et al. report a terbium ion (Tb^{3+})-modified CDs ratiometric fluorescent sensor sensitized by 2,6-pyridinedicarboxylic acid [54]. Upon 290 nm excitation, the sensor exhibits dual emissions: CD emission at 436 nm (response signal) and pyridinedicarboxylic acid/Tb^{3+} complex emission at 543 nm (reference signal). Mercury ion (Hg^{2+}) addition induces significant quenching of the 436 nm emission, while the 543 nm emission remains unaffected. Fluorescence quenching is attributed to ET between CDs and Hg^{2+} ions. The ratiometric fluorescence intensity ratio shows a linear correlation with Hg^{2+} concentrations (1–161.51 μM) and achieves a detection limit of approximately 37 nM. Table 2 summarizes

representative CD-based sensing systems utilizing ET mechanisms for detecting analytes, including various metal ions and small molecules (e.g., glutathione, hydrogen peroxide).

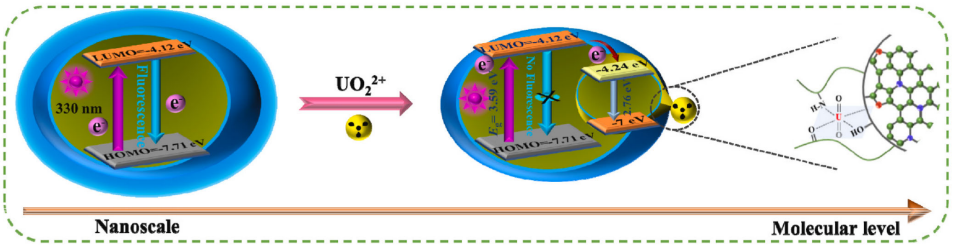


Figure 6. ET mechanism of UO_2^{2+} ion detection [53]. Reproduced from Ref. [53] with permission from Elsevier.

Table 2. Summary of CD detection based on ET mechanism.

Analytes	Linearity Range	Limit of Detection	Reference
Cu^{2+}	0.01–2 μM	6.7 nM	[55]
Ag^{+}	0.1–265 μM	50 nM	[56]
Fe^{3+}	0–2 μM	70 nM	[57]
$ONOO^{-}$	4–120 nM	2.9 nM	[58]
Hg^{2+}	0.05–5 μM	0.02 μM	[59]
N-acetylcysteine	5.56–277.8 μM	0.56 μM	[60]
Glutathione	1–80 μM	83 nM	[61]
Methanal	0–400 μM	0.9 μM	[62]
Peroxide	0–2 μM	84 nM	[63]
Prilocaine	2.3–400 nM	1.8 nM	[64]

3.5. IFE

The IFE represents a significant non-radiative energy conversion mechanism in fluorescence spectroscopy, arising from absorber-mediated attenuation of excitation and/or emission light within the sensing system [65]. Efficient IFE requires spectral overlap between the absorber's absorption band and the luminescent probe's excitation/emission bands [66], enabling broad applicability in chemical and biological sensing. Absorbers competitively absorb excitation/emission photons without altering the intrinsic luminescence properties of the fluorescent material.

IFE-based sensing platforms offer simplicity and versatility, relying solely on spectral matching between CDs and analytes. Zhou et al. report a CD-based sensor for the highly selective and sensitive detection of 2,4,6-trinitrophenol (TNP) [67]. Upon TNP addition, the CDs' fluorescence gradually decreases due to IFE-mediated quenching (Figure 7). The sensor achieved a detection limit of 5.37 ng/mL under optimal conditions and demonstrated satisfactory recovery rates in TNP-spiked water samples, establishing it as a reliable tool for environmental TNP monitoring. Furthermore, Wang et al. developed boron/nitrogen-codoped dual-emission CDs for ratiometric fluorescence detection of hexavalent chromium (Cr^{6+}) ions [68]. Cr^{6+} presence induces significant quenching of emissions centered at (360, 465) nm via IFE, while emissions at (490, 535) nm remain unaffected. The ratiometric response exhibits excellent linearity across 0–100 μM Cr^{6+} concentrations, with a detection limit of 0.41 μM. The multifunctional sensing capabilities of these CDs in real samples not only provide a novel approach for rapid Cr^{6+} determination but also highlight the potential of multi-emissive carbon-based materials in developing ratiometric sensing platforms for diverse analytes. Table 3 summarizes representative CD-based IFE sensing systems targeting metal ions and biomolecules (e.g., alkaline phosphatase, hemin, antibiotics).

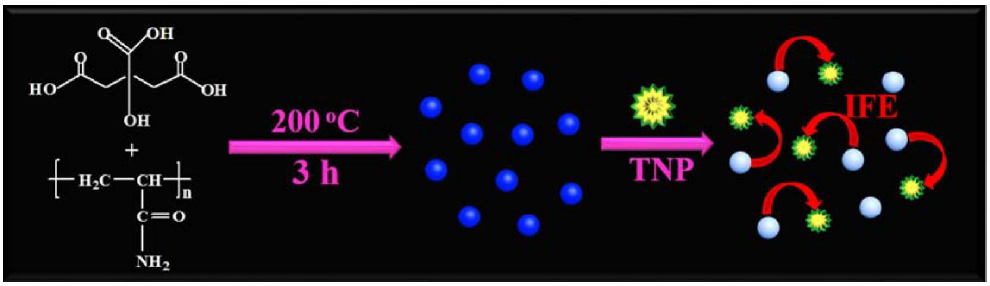


Figure 7. Illustration of the synthesis of the fluorescent CDs and working principle of the sensor [67]. Reproduced from Ref. [67] with permission from Elsevier.

Table 3. Summary of CD detection based on the IFE mechanism.

Analytes	Linearity Range	Limit of Detection	Reference
Hg^{2+}	2–200 nM	0.32 nM	[69]
Ca^{2+}	0.09–14 μM	5 nM	[70]
Cu^{2+}	10–1100 nM	6 nM	[71]
MnO_4^-	0.05–60 μM	13 nM	[72]
Melamine	0.1–20 μM	/	[73]
Alkaline phosphatase	0.01–25 U/L	0.001 U/L	[74]
α-Glucosidase	0.2–10 U/mL	0.01 U/mL	[75]
Vitamin B12	0.25–100 μM	0.14 μM	[76]
Hematin	0.5–10 μM	0.25 μM	[77]
Tetracycline	0.5–200 μM	0.3 μM	[30]
2,4,6-Trinitrophenol	0.1–100 μM	28 nM	[66]

4. Conclusions and Outlook

CDs have demonstrated immense potential as next-generation fluorescent probes in sensing applications due to their unique combination of tunable fluorescence, high QYs, excellent water solubility, and outstanding biocompatibility. These zero-dimensional carbon-based materials exhibit versatile sensing mechanisms including FRET, AIE, ACQ, ET, and IFE, enabling highly sensitive and selective detection of diverse analytes ranging from metal ions to biomolecules. Their superior photostability compared to conventional fluorescent materials, coupled with low toxicity and cost-effective synthesis, makes them particularly attractive for environmental monitoring, biomedical diagnostics, and food safety applications.

Despite significant advancements, several challenges persist. First, while diverse synthetic strategies have been developed, a reliable method for producing structurally homogeneous, high-quality CDs remains elusive, with heterogeneities often compromising sensing performance. Second, the complex structural composition of CDs obscures the precise elucidation of their luminescence mechanisms, hindering predictive synthesis and rational design of CD probes with tailored emission profiles. Furthermore, the prevalence of short-wavelength (e.g., blue) emission in most CDs limits their utility in deep-tissue imaging due to poor tissue penetration.

Looking forward, CD-based sensing systems must prioritize simplicity, miniaturization, and practicality. A critical need exists to transition from in vitro aqueous assays to real-time imaging analyses at cellular, tissue, and in vivo levels. The development of ratiometric or dynamically reversible CD fluorescent probes will be pivotal for achieving reliable, precise, and dynamic analyte detection. Additionally, leveraging CD probes for point-of-care diagnostics and early disease detection represents a transformative frontier. Addressing these challenges demands interdisciplinary efforts to refine synthetic methodologies, decipher optical origins through advanced characterization techniques,

and engineer CDs with tunable emission across the visible-to-NIR spectrum. While obstacles remain, the unique advantages of CDs—including their facile surface functionalization, low toxicity, and versatile photoluminescence—ensure a promising trajectory for their integration into cutting-edge sensing and biomedical technologies.

Author Contributions: Funding acquisition, L.Z. and B.-B.C.; project administration, L.Z. and B.-B.C.; supervision, L.Z. and B.-B.C.; writing—original draft, X.-T.L.; writing—review and editing, B.-B.C. All authors have read and agreed to the published version of the manuscript.

Funding: The authors appreciate the financial support from the Open Fund of Key Laboratory of Luminescence Analysis and Molecular Sensing (Southwest University).

Data Availability Statement: No new data were created or analyzed in this study.

Conflicts of Interest: The authors declare no conflicts of interest.

References

1. Mosconi, D.; Mazzier, D.; Silvestrini, S.; Privitera, A.; Marega, C.; Franco, L.; Moretto, A. Synthesis and photochemical applications of processable polymers enclosing photoluminescent carbon quantum dots. *ACS Nano* **2015**, *9*, 4156–4164. [CrossRef]
2. Tang, Q.; Zhu, W.; He, B.; Yang, P. Rapid conversion from carbohydrates to large-scale carbon quantum dots for all-weather solar cells. *ACS Nano* **2017**, *11*, 1540–1547. [CrossRef]
3. Jeon, S.J.; Kang, T.W.; Ju, J.M.; Kim, M.J.; Park, J.H.; Raza, F.; Han, J.; Lee, H.R.; Kim, J.H. Modulating the photocatalytic activity of graphene quantum dots via atomic tailoring for highly enhanced photocatalysis under visible light. *Adv. Funct. Mater.* **2016**, *26*, 8211–8219. [CrossRef]
4. Chen, H.M.; Wang, G.D.; Tang, W.; Todd, T.; Zhen, Z.P.; Chu, T.; Hekmatyar, K.; Cowger, T.; Hubbard, R.B.; Zhang, W.Z.; et al. Gd-encapsulated carbonaceous dots with efficient renal clearance for magnetic resonance imaging. *Adv. Mater.* **2014**, *26*, 6761–6766. [CrossRef] [PubMed]
5. Lu, S.Y.; Sui, L.Z.; Liu, J.J.; Zhu, S.J.; Chen, A.M.; Jin, M.X.; Yang, B. Near-infrared photoluminescent polymer-carbon nanodots with two-photon fluorescence. *Adv. Mater.* **2017**, *29*, 1603443. [CrossRef]
6. Liu, H.P.; Ye, T.; Mao, C.D. Fluorescent carbon nanoparticles derived from candle soot. *Angew. Chem. Int. Ed.* **2007**, *46*, 6473–6475. [CrossRef] [PubMed]
7. Peng, J.; Gao, W.; Gupta, B.K.; Liu, Z.; Romero-Aburto, R.; Ge, L.H.; Song, L.; Alemany, L.B.; Zhan, X.B.; Gao, G.H.; et al. Graphene quantum dots derived from carbon fibers. *Nano Lett.* **2012**, *12*, 844–849. [CrossRef]
8. Liu, F.; Jang, M.H.; Ha, H.D.; Kim, J.H.; Cho, Y.H.; Seo, T.S. Facile synthetic method for pristine graphene quantum dots and graphene oxide quantum dots: Origin of blue and green luminescence. *Adv. Mater.* **2013**, *25*, 3657–3662. [CrossRef]
9. Liu, M.L.; Chen, B.B.; Li, C.M.; Huang, C.Z. Carbon dots: Synthesis, formation mechanism, fluorescence origin and sensing applications. *Green Chem.* **2019**, *21*, 449–471. [CrossRef]
10. Lou, Q.; Chen, N.; Zhu, J.; Liu, K.; Li, C.; Zhu, Y.; Xu, W.; Chen, X.; Song, Z.; Liang, C.; et al. Thermally enhanced and long lifetime red TADF carbon dots via multi-confinement and phosphorescence assisted energy transfer. *Adv. Mater.* **2023**, *35*, 2211858. [CrossRef]
11. Sun, H.; Xia, P.; Shao, H.; Zhang, R.; Lu, C.; Xu, S.; Wang, C. Heating-free synthesis of red emissive carbon dots through separated processes of polymerization and carbonization. *J. Colloid Interface Sci.* **2023**, *646*, 932–939. [CrossRef]
12. Chen, B.-B.; Liu, M.-L.; Gao, Y.-T.; Chang, S.; Qian, R.-C.; Li, D.-W. Design and applications of carbon dots-based ratiometric fluorescent probes: A review. *Nano Res.* **2023**, *16*, 1064–1083. [CrossRef]
13. Xia, C.; Zhu, S.; Feng, T.; Yang, M.; Yang, B. Evolution and synthesis of carbon dots: From carbon dots to carbonized polymer dots. *Adv. Sci.* **2019**, *6*, 1901316. [CrossRef]
14. Siraj, N.; El-Zahab, B.; Hamdan, S.; Karam, T.E.; Haber, L.H.; Li, M.; Fakayode, S.O.; Das, S.; Valle, B.; Strongin, R.M.; et al. Fluorescence, phosphorescence, and chemiluminescence. *Anal. Chem.* **2016**, *88*, 170–202. [CrossRef] [PubMed]
15. Liu, M.L.; Chen, B.B.; Li, C.M.; Huang, C.Z. Carbon dots prepared for fluorescence and chemiluminescence sensing. *Sci. China Chem.* **2019**, *62*, 968–981. [CrossRef]
16. Zhu, S.J.; Zhang, J.H.; Tang, S.J.; Qiao, C.Y.; Wang, L.; Wang, H.Y.; Liu, X.; Li, B.; Li, Y.F.; Yu, W.L.; et al. Surface chemistry routes to modulate the photoluminescence of graphene quantum dots: From fluorescence mechanism to up-conversion bioimaging applications. *Adv. Funct. Mater.* **2012**, *22*, 4732–4740. [CrossRef]
17. Sun, Y.P.; Zhou, B.; Lin, Y.; Wang, W.; Fernando, K.A.S.; Pathak, P.; Meziani, M.J.; Harruff, B.A.; Wang, X.; Wang, H.F.; et al. Quantum-sized carbon dots for bright and colorful photoluminescence. *J. Am. Chem. Soc.* **2006**, *128*, 7756–7757. [CrossRef] [PubMed]

18. Chen, B.B.; Liu, M.L.; Li, C.M.; Huang, C.Z. Fluorescent carbon dots functionalization. *Adv. Colloid Interface Sci.* **2019**, *270*, 165–190. [CrossRef]
19. Wang, Z.F.; Yuan, F.L.; Li, X.H.; Li, Y.C.; Zhong, H.Z.; Fan, L.Z.; Yang, S.H. 53% Efficient red emissive carbon quantum dots for high color rendering and stable warm white-light-emitting diodes. *Adv. Mater.* **2017**, *29*, 1702910. [CrossRef]
20. Chekini, M.; Prince, E.; Zhao, L.; Mundoor, H.; Smalyukh, I.I.; Kumacheva, E. Chiral carbon dots synthesized on cellulose nanocrystals. *Adv. Opt. Mater.* **2020**, *8*, 1901911. [CrossRef]
21. Kang, C.; Tao, S.; Yang, F.; Yang, B. Aggregation and luminescence in carbonized polymer dots. *Aggregate* **2022**, *3*, e169. [CrossRef]
22. Liu, M.L.; Yang, L.; Li, R.S.; Chen, B.B.; Liu, H.; Huang, C.Z. Large-scale simultaneous synthesis of highly photoluminescent green amorphous carbon nanodots and yellow crystalline graphene quantum dots at room temperature. *Green Chem.* **2017**, *19*, 3611–3617. [CrossRef]
23. Park, Y.; Yoo, J.; Lim, B.; Kwon, W.; Rhee, S.W. Improving the functionality of carbon nanodots: Doping and surface functionalization. *J. Mater. Chem. A* **2016**, *4*, 11582–11603. [CrossRef]
24. Liu, M.L. Optical properties of carbon dots: A review. *Nanoarchitectonics* **2019**, *1*, 1–12. [CrossRef]
25. Zhu, S.J.; Song, Y.B.; Zhao, X.H.; Shao, J.R.; Zhang, J.H.; Yang, B. The photoluminescence mechanism in carbon dots (graphene quantum dots, carbon nanodots, and polymer dots): Current state and future perspective. *Nano Res.* **2015**, *8*, 355–381. [CrossRef]
26. Sudolská, M.; Dubecký, M.; Sarkar, S.; Reckmeier, C.J.; Zbořil, R.; Rogach, A.L.; Otyepka, M. Nature of absorption bands in oxygen-functionalized graphitic carbon dots. *J. Phys. Chem. C* **2015**, *119*, 13369–13373. [CrossRef]
27. Zhu, J.Y.; Bai, X.; Bai, J.L.; Pan, G.C.; Zhu, Y.S.; Zhai, Y.; Shao, H.; Chen, X.; Dong, B.; Zhang, H.Z.; et al. Emitting color tunable carbon dots by adjusting solvent towards light-emitting devices. *Nanotechnology* **2018**, *29*, 085705. [CrossRef]
28. Wang, Y.; Kalytchuk, S.; Zhang, Y.; Shi, H.C.; Kershaw, S.V.; Rogach, A.L. Thickness-dependent full-color emission tunability in a flexible carbon dot ionogel. *J. Phys. Chem. Lett.* **2014**, *5*, 1412–1420. [CrossRef] [PubMed]
29. Chen, D.Q.; Wu, W.W.; Yuan, Y.J.; Zhou, Y.; Wan, Z.Y.; Huang, P. Intense multi-state visible absorption and full-color luminescence of nitrogen-doped carbon quantum dots for blue-light-excitable solid-state-lighting. *J. Mater. Chem. C* **2016**, *4*, 9027–9035. [CrossRef]
30. Liu, M.L.; Chen, B.B.; Yang, T.; Wang, J.; Liu, X.D.; Huang, C.Z. One-pot carbonization synthesis of europium-doped carbon quantum dots for highly selective detection of tetracycline. *Methods Appl. Fluoresc.* **2017**, *5*, 015003. [CrossRef]
31. Liu, M.L.; Chen, B.B.; He, J.H.; Li, C.M.; Li, Y.F.; Huang, C.Z. Anthrax biomarker: An ultrasensitive fluorescent ratiometry of dipicolinic acid by using terbium(III)-modified carbon dots. *Talanta* **2019**, *191*, 443–448. [CrossRef]
32. Ding, H.; Yu, S.B.; Wei, J.S.; Xiong, H.M. Full-color light-emitting carbon dots with a surface-state-controlled luminescence mechanism. *ACS Nano* **2016**, *10*, 484–491. [CrossRef]
33. Kim, S.; Hwang, S.W.; Kim, M.K.; Dong, Y.S.; Dong, H.S.; Chang, O.K.; Yang, S.B.; Park, J.H.; Hwang, E.; Choi, S.H.; et al. Anomalous behaviors of visible luminescence from graphene quantum dots: Interplay between size and shape. *ACS Nano* **2012**, *6*, 8203–8208. [CrossRef]
34. Cao, L.; Meziani, M.J.; Sahu, S.; Sun, Y.P. Photoluminescence properties of graphene versus other carbon nanomaterials. *Acc. Chem. Res.* **2013**, *46*, 171–180. [CrossRef] [PubMed]
35. Sun, M.; Liang, M.; Kong, R.; Guo, L.; Xia, L.; Qu, F. FRET-based dual-color carbon dot ratiometric fluorescent sensor enables the smartphone-integrated device for noninvasive and portable diagnosis of chronic kidney disease. *Anal. Chem.* **2024**, *96*, 17907–17913. [CrossRef] [PubMed]
36. Qu, J.; Zhang, X.; Zhou, W.; Yao, R.; Zhang, X.; Jing, S. Carbon dots/Ruthenium(III) nanocomposites for FRET fluorescence detection and removal of mercury (II) via assembling into nanofibers. *Talanta* **2024**, *268*, 125322. [CrossRef]
37. Nayak, S.; Banerjee, S.; Kamra, A.; Das, P.; Rana, S. Carbon-nanodot-based bicontinuous particles for FRET-based pH sensing. *ACS Appl. Nano Mater.* **2024**, *7*, 25261–25269. [CrossRef]
38. Ganiga, M.; Cyriac, J. FRET based ammonia sensor using carbon dots. *Sens. Actuators B-Chem.* **2016**, *225*, 522–528. [CrossRef]
39. Sotolongo-García, R.; Rodríguez-Velázquez, E.; Alatorre-Meda, M.; Oropeza-Guzmán, M.T.; Tirado-Guízar, A.; Pina-Luis, G. Optimizing the efficiency of a cytocompatible carbon-dots-based FRET platform and its application as a riboflavin sensor in beverages. *Nanomaterials* **2021**, *11*, 1981. [CrossRef]
40. Zhao, X.E.; Lei, C.H.; Gao, Y.; Gao, H.; Zhu, S.Y.; Yang, X.; You, J.m.; Wang, H. A ratiometric fluorescent nanosensor for the detection of silver ions using graphene quantum dots. *Sens. Actuators B-Chem.* **2017**, *253*, 239–246. [CrossRef]
41. Yu, X.; Zhang, C.X.; Zhang, L.N.; Xue, Y.R.; Li, H.W.; Wu, Y.Q. The construction of a FRET assembly by using gold nanoclusters and carbon dots and their application as a ratiometric probe for cysteine detection. *Sens. Actuators B-Chem.* **2018**, *263*, 327–335. [CrossRef]
42. Rong, M.C.; Liang, Y.C.; Zhao, D.L.; Chen, B.J.; Pan, C.; Deng, X.Z.; Chen, Y.B.; He, J. A ratiometric fluorescence visual test paper for an anthrax biomarker based on functionalized manganese-doped carbon dots. *Sens. Actuators B-Chem.* **2018**, *265*, 498–505. [CrossRef]

43. Yang, W.Q.; Ni, J.C.; Luo, F.; Weng, W.; Wei, Q.H.; Lin, Z.Y.; Chen, G.N. Cationic carbon dots for modification-free detection of hyaluronidase via an electrostatic-controlled ratiometric fluorescence assay. *Anal. Chem.* **2017**, *89*, 8384–8390. [CrossRef]
44. Hou, J.Y.; Tian, Z.b.; Xie, H.z.; Tian, Q.y.; Ai, S.y. A fluorescence resonance energy transfer sensor based on quaternized carbon dots and Ellman's test for ultrasensitive detection of dichlorvos. *Sens. Actuators B-Chem.* **2016**, *232*, 477–483. [CrossRef]
45. Luo, J.; Xie, Z.; Lam, J.W.Y.; Cheng, L.; Chen, H.; Qiu, C.; Kwok, H.S.; Zhan, X.; Liu, Y.; Zhu, D.; et al. Aggregation-induced emission of 1-methyl-1,2,3,4,5-pentaphenylsilole. *Chem. Commun.* **2001**, *18*, 1740–1741. [CrossRef] [PubMed]
46. Liu, J.; Zhan, Y.; Qiu, B.; Lin, Z.; Guo, L. Portable smartphone platform based on aggregation-induced enhanced emission carbon dots for ratiometric quantitative sensing of fluoride ions. *ACS Sens.* **2023**, *8*, 884–892. [CrossRef]
47. Zhang, S.; Li, B.; Zhou, J.; Shi, J.; He, Z.; Zhao, Y.; Li, Y.; Shen, Y.; Zhang, Y.; Wu, S. Kill three birds with one stone: Mitochondria-localized tea saponin derived carbon dots with AIE properties for stable detection of HSA and extremely acidic pH. *Food Chem.* **2023**, *405*, 134865. [CrossRef]
48. Kawamura, Y.; Brooks, J.; Brown, J.J.; Sasabe, H.; Adachi, C. Intermolecular Interaction and a Concentration-Quenching Mechanism of Phosphorescent Ir(III) Complexes in a Solid Film. *Phys. Rev. Lett.* **2006**, *96*, 017404. [CrossRef]
49. Tai, K.; Lü, W.; Umezu, I.; Sugimura, A. Inter-Dot Distance Dependence of Photoluminescence Properties in CdSe Quantum Dot Systems. *Appl. Phys. Express* **2010**, *3*, 035202. [CrossRef]
50. Chen, S.; Liu, J.W.; Chen, M.L.; Chen, X.W.; Wang, J.H. Unusual emission transformation of graphene quantum dots induced by self-assembled aggregation. *Chem. Commun.* **2012**, *48*, 7637–7639. [CrossRef] [PubMed]
51. Bhattacharya, S.; Sarkar, R.; Nandi, S.; Porgador, A.; Jelinek, R. Detection of reactive oxygen species by a carbon-dot–ascorbic acid hydrogel. *Anal. Chem.* **2017**, *89*, 830–836. [CrossRef] [PubMed]
52. Wang, N.; Liu, Z.X.; Li, R.S.; Zhang, H.Z.; Huang, C.Z.; Wang, J. The aggregation induced emission quenching of graphene quantum dots for visualizing the dynamic invasions of cobalt(ii) into living cells. *J. Mater. Chem. B* **2017**, *5*, 6394–6399. [CrossRef] [PubMed]
53. Wang, Q.; Zhang, H.; Yu, D.; Qin, W.; Wu, X. Ultra-sensitive and stable N-doped carbon dots for selective detection of uranium through electron transfer induced UO2+(V) sensing mechanism. *Carbon* **2022**, *198*, 162–170. [CrossRef]
54. He, X.; Han, Y.; Luo, X.; Yang, W.; Li, C.; Tang, W.; Yue, T.; Li, Z. Terbium (III)-referenced N-doped carbon dots for ratiometric fluorescent sensing of mercury (II) in seafood. *Food Chem.* **2020**, *320*, 126624. [CrossRef] [PubMed]
55. Wang, J.; Li, R.S.; Zhang, H.Z.; Wang, N.; Zhang, Z.; Huang, C.Z. Highly fluorescent carbon dots as selective and visual probes for sensing copper ions in living cells via an electron transfer process. *Biosens. Bioelectron.* **2017**, *97*, 157–163. [CrossRef] [PubMed]
56. Liu, G.L.; Xuan, C.L.; Feng, D.Q.; Hua, D.L.; Liu, T.H.; Qi, G.; Wang, W. Dual-modal fluorescence and light-scattering sensor based on water-soluble carbon dots for silver ions detection. *Anal. Methods* **2017**, *9*, 5611–5617. [CrossRef]
57. Atchudan, R.; Edison, T.N.J.I.; Chakradhar, D.; Perumal, S.; Shim, J.J.; Lee, Y.R. Facile green synthesis of nitrogen-doped carbon dots using Chionanthus retusus fruit extract and investigation of their suitability for metal ion sensing and biological applications. *Sens. Actuators B-Chem.* **2017**, *246*, 497–509. [CrossRef]
58. Zhu, J.L.; Sun, S.; Jiang, K.; Wang, Y.H.; Liu, W.Q.; Lin, H.W. A highly sensitive and selective fluorimetric probe for intracellular peroxynitrite based on photoinduced electron transfer from ferrocene to carbon dots. *Biosens. Bioelectron.* **2017**, *97*, 150–156. [CrossRef]
59. Liu, T.; Li, N.; Dong, J.X.; Luo, H.Q.; Li, N.B. Fluorescence detection of mercury ions and cysteine based on magnesium and nitrogen co-doped carbon quantum dots and IMPLICATION logic gate operation. *Sens. Actuators B-Chem.* **2016**, *231*, 147–153. [CrossRef]
60. Liu, H.; Li, R.S.; Zhou, J.; Huang, C.Z. Branched polyethylenimine-functionalized carbon dots as sensitive and selective fluorescent probes for N-acetylcysteine via an off-on mechanism. *Analyst* **2017**, *142*, 4221–4227. [CrossRef]
61. Meng, H.-M.; Zhao, D.; Li, N.; Chang, J. A graphene quantum dot-based multifunctional two-photon nanoprobe for the detection and imaging of intracellular glutathione and enhanced photodynamic therapy. *Analyst* **2018**, *143*, 4967–4973. [CrossRef] [PubMed]
62. Liu, H.; Sun, Y.; Li, Z.; Yang, J.; Aryee, A.A.; Qu, L.; Du, D.; Lin, Y. Lysosome-targeted carbon dots for ratiometric imaging of formaldehyde in living cells. *Nanoscale* **2019**, *11*, 8458–8463. [CrossRef]
63. Lan, M.; Di, Y.; Zhu, X.; Ng, T.-W.; Xia, J.; Liu, W.; Meng, X.; Wang, P.; Lee, C.-S.; Zhang, W. A carbon dot-based fluorescence turn-on sensor for hydrogen peroxide with a photo-induced electron transfer mechanism. *Chem. Commun.* **2015**, *51*, 15574–15577. [CrossRef]
64. Ensafi, A.A.; Sefat, S.H.; Kazemifard, N.; Rezaei, B.; Moradi, F. A novel one-step and green synthesis of highly fluorescent carbon dots from saffron for cell imaging and sensing of prilocaine. *Sens. Actuators B-Chem.* **2017**, *253*, 451–460. [CrossRef]
65. Chen, S.; Yu, Y.L.; Wang, J.H. Inner filter effect-based fluorescent sensing systems: A review. *Anal. Chim. Acta* **2018**, *999*, 13–26. [CrossRef]
66. Liu, M.L.; Chen, B.B.; Liu, Z.X.; Huang, C.Z. Highly selective and sensitive detection of 2,4,6-trinitrophenol by using newly developed blue–green photoluminescent carbon nanodots. *Talanta* **2016**, *161*, 875–880. [CrossRef]

67. Wang, X.; Liu, Y.; Zhou, Q.; Sheng, X.; Sun, Y.; Zhou, B.; Zhao, J.; Guo, J. A reliable and facile fluorescent sensor from carbon dots for sensing 2,4,6-trinitrophenol based on inner filter effect. *Sci. Total Environ.* **2020**, *720*, 137680. [CrossRef]
68. Jia, M.; Peng, L.; Yang, M.; Wei, H.; Zhang, M.; Wang, Y. Carbon dots with dual emission: A versatile sensing platform for rapid assay of Cr (VI). *Carbon* **2021**, *182*, 42–50. [CrossRef]
69. Peng, D.; Zhang, L.; Liang, R.P.; Qiu, J.D. Rapid detection of mercury ions based on nitrogen-doped graphene quantum dots accelerating formation of manganese porphyrin. *ACS Sens.* **2018**, *3*, 1040–1047. [CrossRef] [PubMed]
70. Chen, D.; Zhao, J.; Zhang, L.; Liu, R.; Huang, Y.; Lan, C.; Zhao, S. Capsicum-derived biomass quantum dots coupled with alizarin red S as an inner-filter-mediated illuminant nanosystem for imaging of intracellular calcium ions. *Anal. Chem.* **2018**, *90*, 13059–13064. [CrossRef] [PubMed]
71. Dong, Y.; Wang, R.; Li, G.; Chen, C.; Chi, Y.; Chen, G. Polyamine-functionalized carbon quantum dots as fluorescent probes for selective and sensitive detection of copper ions. *Anal. Chem.* **2012**, *84*, 6220–6224. [CrossRef]
72. Jiang, X.; Qin, D.; Mo, G.; Feng, J.; Zheng, X.; Deng, B. Facile preparation of boron and nitrogen codoped green emission carbon quantum dots for detection of permanganate and captopril. *Anal. Chem.* **2019**, *91*, 11455–11460. [CrossRef] [PubMed]
73. Wang, T.Y.; Chen, C.Y.; Wang, C.M.; Tan, Y.Z.; Liao, W.S. Multicolor functional carbon dots via one-step refluxing synthesis. *ACS Sens.* **2017**, *2*, 354–363. [CrossRef] [PubMed]
74. Li, G.L.; Fu, H.L.; Chen, X.J.; Gong, P.W.; Chen, G.; Xia, L.; Wang, H.; You, J.M.; Wu, Y.N. Facile and sensitive fuorescence sensing of alkaline phosphatase activity with photoluminescent carbon dots based on inner filter effect. *Anal. Chem.* **2016**, *88*, 2720–2726. [CrossRef] [PubMed]
75. Kong, W.H.; Wu, D.; Xia, L.; Chen, X.F.; Li, G.L.; Qiu, N.N.; Chen, G.; Sun, Z.W.; You, J.M.; Wu, Y.N. Carbon dots for fluorescent detection of α-glucosidase activity using enzyme activated inner filter effect and its application to anti-diabetic drug discovery. *Anal. Chim. Acta* **2017**, *973*, 91–99. [CrossRef]
76. Gao, Y.-T.; Chen, B.-B.; Jiang, L.; Lv, J.; Chang, S.; Wang, Y.; Qian, R.-C.; Li, D.-W.; Hafez, M.-E. Dual-emitting carbonized polymer dots synthesized at room temperature for ratiometric fluorescence sensing of vitamin B12. *ACS Appl. Mater. Interfaces* **2021**, *13*, 50228–50235. [CrossRef]
77. Zhang, Q.Q.; Chen, B.B.; Zou, H.Y.; Li, Y.F.; Huang, C.Z. Inner filter with carbon quantum dots: A selective sensing platform for detection of hematin in human red cells. *Biosens. Bioelectron.* **2018**, *100*, 148–154. [CrossRef]

Disclaimer/Publisher's Note: The statements, opinions and data contained in all publications are solely those of the individual author(s) and contributor(s) and not of MDPI and/or the editor(s). MDPI and/or the editor(s) disclaim responsibility for any injury to people or property resulting from any ideas, methods, instructions or products referred to in the content.